



Published in final edited form as:

Curr Opin Chem Biol. 2008 December ; 12(6): 626–639. doi:10.1016/j.cbpa.2008.10.005.

Experimental analyses of the chemical dynamics of ribozyme catalysis

Michael E Harris¹ and Adam G Cassano²

¹RNA Center and Department of Biochemistry, Case Western Reserve University School of Medicine, Cleveland OH 44118

²Department of Chemistry, Drew University, Madison NJ 07940

Abstract

Most ribozymes in Nature catalyze alcoholysis or hydrolysis of RNA phosphodiester bonds. Studies of the corresponding non-enzymatic reactions reveal a complex mechanistic landscape allowing for a variety of transition states and both concerted and step-wise mechanisms. High resolution structures, incisive biochemical studies and computer simulations are providing glimpses into how ribozyme catalyzed reactions traverse this landscape. However, direct experimental tests of such mechanistic detail at the chemical level are not easily achieved. Kinetic isotope effects (KIEs) probe directly the differences in the vibrational “environment” of the atoms undergoing chemical transformation on going from the ground state to the transition state. Thus, KIEs can in principle provide direct information about transition state bonding and so may be instrumental in evaluating possible transition states for ribozyme catalyzed reactions. Understanding charge distribution in the transition state may help resolve how rate acceleration is accomplished and perhaps the similarities and differences in how RNA and protein active sites operate. Several barriers to successful application of KIE analysis to ribozymes have recently been overcome, and new chemical details are beginning to emerge.

Introduction

Protein and RNA enzymes (ribozymes) are dynamic and undergo motions with a variety of magnitudes and time scales. The ultimate expression of these motions is the facilitation of bond fission and formation via “catalytic” interactions between ribozyme active site residues and substrate atoms that enhance chemical reactivity. Thus, in addition to defining the dynamic behavior of ribozymes at a molecular level it is essential to understand the chemical dynamics of the reactions they catalyze, and to define the interactions occurring between ribozyme and substrate that promote chemical transformation. Aside from the ribosome, most RNA enzymes catalyze phosphoryl transfer reactions and this article focuses on this main ribozyme class. The catalysis of acyl transfer by large subunit ribosomal RNA is clearly of high intrinsic interest—important progress has been made and detailed reviews are available [1–3]. Phosphoryl transfer ribozymes can be grouped into two classes based on mechanism [4,5]: Large ribozymes catalyze the displacement of the 3' O from an RNA 3',5'-phosphodiester by intermolecular reactions using water or a ribose 2' or 3' hydroxyl as the nucleophile, and Small ribozymes

Correspondence: MEH: phone- (216) 368-4779, email- michael.e.harris@case.edu; AGC: phone- (973) 408-3341, email- acassano@drew.edu.

Publisher's Disclaimer: This is a PDF file of an unedited manuscript that has been accepted for publication. As a service to our customers we are providing this early version of the manuscript. The manuscript will undergo copyediting, typesetting, and review of the resulting proof before it is published in its final citable form. Please note that during the production process errors may be discovered which could affect the content, and all legal disclaimers that apply to the journal pertain.

catalyze the displacement of the 5' O from an RNA phosphodiester by an intramolecular reaction involving the adjacent 2' OH as the nucleophile (Figure 1). It has become clear that divalent metal ions play key roles in catalysis by both classes. Importantly, research on Small ribozymes shows that they can work efficiently in the absence of metals and the focus of understanding their catalytic prowess is justifiably on acid/base catalytic mechanisms. Thus, as with most enzyme-catalyzed addition/displacement reactions the important questions for ribozyme catalysis essentially boil down to the following: Is the reaction concerted or stepwise; what is the structure of transition states between precursor and product; what is the timing and trajectory of proton transfers (what groups donate / what groups accept); and how do active site metal ions, when present, contribute to catalysis?

Answers for these questions are emerging from high resolution structures, detailed biochemical and physical experimentation and *in silico* simulation [4–8]. In principle, the most direct approach for probing transition state (TS) structure and for understanding how active site interactions might influence its charge distribution is the determination of kinetic effects that arise from isotopic substitution of the reacting atoms (e.g. [9–11]). Substituting individual atoms with heavier, stable isotopes affects the rates and equilibria of chemical reactions in ways that reflect changes in the bonding environment of the substituted atom on going from the ground state to the TS. Indeed, extensive application of KIEs to analysis of phosphodiester reaction mechanisms in solution provides a framework for interpreting isotope effects for reactions that occur on enzymes. However, substituting one of the 600 or so atoms in a small (20 nt) oligonucleotide of RNA with a different isotope of that atom is non-trivial and the effects of such substitutions on reaction rate, though information-rich, are very small in magnitude. As a result, specialized methods are necessary to measure them. Now, there is progress in meeting these challenges, and information on the detailed chemical mechanisms of ribozyme catalysis is beginning to emerge.

The mechanistic landscape for biological phosphoryl transfer

The mechanisms by which transition state stabilization may be accomplished by ribozymes or any other catalyst are dictated by the intrinsic chemical properties of the reacting organic molecules [12,13]. Extensive research on reactions of phosphate esters with nucleophiles show they may react by a continuum of TSs defined primarily by the extent of bond formation to the nucleophile and the extent of bond fission to the leaving group (Figure 2). These two coordinates together define a conformational landscape for the TS, which can be visualized by what is often referred to as a More-O'Ferrel/Jencks (MOJ) diagram, where changes in bond order to the nucleophile define one axis and changes in bond order to the leaving group define the other (e.g. [14,15]). The precursor diester defines one corner (lower left) and the hydrolyzed or transferred product is located on the opposite, or diagonal, corner (upper right). These two states are connected by the reaction coordinate.

Both diagonals of the diagram describe specific attributes of TS structure. The diagonal between the phosphorane and metaphosphate structures can be considered as the “tightness coordinate” defining whether a TS lies close to the dissociative, metaphosphate limit (“loose”) or is closer to the associative, phosphorane limit (“tight”) [16]. The opposite diagonal, which could be called the “progress coordinate” defines whether the TS is “early” or “late”, depending on whether the TS is closer in electronic character to the precursor or product, respectively. Thus, for a concerted reaction there is a single TS that represents the lowest barrier between the precursor and product. The structure of this TS with respect to O-P bonding is defined by its position along the nucleophile bond formation and leaving group bond cleavage coordinates. Overall TS charge distribution can also be described as early/late, or loose/tight (or associative/dissociative) depending on the synchrony of nucleophilic attack and leaving group departure.

Phosphodiester reactions can have a two-step reaction coordinate, in particular when nucleophilic attack is intramolecular that proceeds first with nucleophilic attack via progress along Nu bond formation coordinate and forms a phosphorane intermediate that, by definition, occupies a local minima on the energy landscape. Breakdown of the intermediate occurs via a second TS to form the hydrolyzed or transferred product. The reactions of RNA in solution also exemplifies this phenomenon (Figure 3). For RNA the predominant reaction at $\text{pH} > 7$ is the hydroxide ion catalyzed transesterification to a 2',3'-cyclic phosphate with release of the 5'O. At $\text{pH} < 7$, pH-independent transesterification to a 2',5'-phosphate (isomerization) is accompanied by slower cleavage to a 2',3'-cyclic phosphate. Given that isomerization occurs via pseudorotation of a phosphorane intermediate, these results suggest that protonation on a non-bridging phosphoryl oxygen is necessary for the stability of the phosphorane intermediate. As no isomerization occurs at $\text{pH} > 7$, the base-catalyzed reaction is thought to occur via a concerted mechanism with an anionic TS.

Mechanistic insight from linear free energy relationships

Experimental insight into mechanism and where the TSs of phosphoryl transfer reactions may lie on the energetic landscape defined by the MOJ diagram comes from analyzing the dependence of reaction rate on nucleophile and leaving group pKa. Such experiments, termed linear free energy relationship (LFER) analyses, highlight that differences in the reactivity of the reacting atoms influence phosphoryl transfer TS structure and mechanism. The second order rate constants for the intermolecular reactions of phosphodiester with nucleophiles strongly depend on leaving group pK_a and nucleophile pK_a with Bronsted values (the slope of $\log k/k_0$ versus pK_a) of $\beta_{\text{lg}} = -1.3$ and $\beta_{\text{nuc}} = 0.3 - 0.47$ (e.g. [16–18]). In LFER studies the comparison of the β value to the substituent effect on the overall reaction equilibrium (β_{eq}) provides an estimation of the effective charge on the reacting group in the TS, and thus the change in bond order [19,20]. For example, experiments using aryl esters the β_{eq} is -1.74 . Given that the leaving group charge in the phenolate product is -1.0 , the ground state charge is considered to be $+0.74$. The β_{lg} for these reactions is -1.3 indicating that leaving group charge in the TS is $-0.6(+0.74 - 1.3)$. Such a result shows a TS that is relatively late with respect to bond cleavage. For nucleophilic attack the observed pKa dependence must be corrected for desolvation, which becomes less favorable as the pKa increases [18] and references therein). Nucleophilic attack by substituted pyridines gives a corrected β_{nuc} of 0.56 and compared an overall β_{eq} of 1.6 the results indicate a TS that is early with respect to nucleophile bond formation. When the leaving group is sulfur instead of oxygen a decrease in β_{nuc} is observed (corrected values of 0.42 versus 0.56, for SP and OP diesters, respectively) providing evidence that the more reactive SP diesters require less nucleophile bonding to achieve the same degree of leaving group bond cleavage [22].

Additional evidence for how changes in reactant structure and reactivity influence TS structure comes LFER analysis of intramolecular reactions of uridine-3'-alkyl- and aryl-phosphodiester. For example, a lesser β_{lg} of -0.54 to -0.59 observed for base catalyzed 2'O-transphosphorylation of uridine aryl phosphates [20,21] relative to intermolecular phosphodiester reactions that also have good leaving groups (see above, $\beta_{\text{lg}} = -1.3$). This observation supports an earlier TS for intramolecular nucleophilic attack with respect to leaving group bond fission relative. Interestingly the β_{lg} is larger for alkyl-diester compared to their aryl counterparts (-1.29 versus -0.54 , for alkyl and aryl-diester, respectively) (e.g. [22]). The fact that no isomerization is seen under these conditions for either group of reactants is evidence in favor of a concerted rather than step-wise mechanism. Given the different β_{lg} measured for alkaline hydrolysis of uridine phosphoalkyl versus aryl esters plotting the data for both classes gives rise to a convex Bronsted plot with inflection at ca. pH 12. Formally the convex plot could be due to a change from a concerted to a stepwise mechanism (but without a sufficiently long lived intermediate to allow pseudorotation), or represent a change in rate limiting step.

For example, the phenol leaving groups nucleophilic attack could be rate limiting, while for the alkoxide leaving groups, the second step of leaving group bond fission could be rate limiting giving rise to a change in β_{lg} . Nonetheless, these studies highlight the need to better understand how changes in nucleophile and leaving group reactivity influence the energetic landscape that defines the reaction mechanism.

Kinetic Isotope effects on phosphoryl transfer reactions

Although highly informative, LFER analyses of TS structure are difficult to apply to enzyme reactions because of their high degree of substrate specificity. Experimental insight into the chemical details of phosphoryl transfer reactions that is demonstrably applicable to exploring ribozyme chemical mechanism is the analysis of kinetic isotope effects. Perturbation of rate and equilibrium constants for a chemical reaction by isotopic substitution has long been used as a mechanistic probe [10,11,23–26]. Extensive reviews of isotope effects and their application to phosphoryl transfer are available [26–28]. In this section, we will focus on how isotope effects for phosphodiester cleavage reactions provide information regarding where the TS lies on the MOJ landscape and thus set the stage for interpretation of effects on enzyme systems such as ribozymes.

Substitution of reacting atoms with heavier, stable isotopes can perturb both the rates and equilibria of the corresponding reactions[29]. Changes in the rates of reactions are referred to as kinetic isotope effects (KIE) and are expressed as the ratio of the rate constant of the lighter isotope to the rate constant of the heavier isotope, k_L/k_H . Thus if the lighter isotope is favored, the isotope effect is greater than unity, and termed “normal.” If, on the other hand, the heavier isotope is favored, the observed isotope effect is less than unity and termed “inverse.” As depicted in Figure 4 heavier isotopes result in lower bond vibrational frequencies due to their increased mass. Two factors contribute to the extent to which differences in vibrational properties influence the observed KIE [30,31]. One factor is determined by the differences in the imaginary frequency of the TS induced by the different masses of the isotopes. The vibration associated with reaction coordinate motion is considered imaginary because it has no restoring force in the TS (symbolized by the inverted hyperbole in Figure 4A). This effect does not change with temperature, and is therefore referred to as the temperature independent factor (TIF), or imaginary frequency factor. The lighter isotope will always possess the greater frequency for the imaginary vibration, and therefore the TIF always favors the lighter isotope, making a normal contribution to the observed isotope effect. The second factor is determined by the changes in the vibrational force constants experienced by the atom of interest as it proceeds from the ground state to the TS (Figure 4B). The magnitude of this factor is influenced by temperature, and correspondingly it is referred to as the temperature dependent factor (TDF). For the TDF, an increase in bond stiffness (bond formation) favors the heavier isotope and decreases in bond stiffness (bond breaking) favor the lighter isotope. Thus, the TDF can make either a normal or inverse contribution to the observed KIE, depending on whether the atom of interest experiences an increase or decrease in bonding.

Factors influencing the magnitude of observed KIEs

In phosphodiester cleavage, the bond to the leaving group oxygen atom is broken, and therefore both the TIF and TDF contribute normally, leading to only normal isotope effects in this position ranging from 1.00 – 1.07 depending on the extent of bond cleavage [32][9]. The overall magnitude of the KIE provides information on the extent of bond cleavage in the TS, and therefore a large $^{18}k_{LG}$ shows that the TS lies in the late portion of the MOJ diagram with respect to leaving group bonding (Figure 5). For the nucleophile a new bond is being formed and the TDF makes an inverse contribution. This inverse contribution competes with the normal TIF contribution to determine whether the overall $^{18}k_{NUC}$ is normal or inverse. In the early and dissociative portions of the MOJ diagram, where bond formation to the nucleophile is not well

advanced the TIF contribution is greater in magnitude than the TDF, leading to a normal $^{18}k_{\text{NUC}}$. In contrast, the late and associative portions of the MOJ diagram represent TSs where bonding to the nucleophile is well advanced, leading to a large inverse contribution from the TDF and an inverse $^{18}k_{\text{NUC}}$. Experimentally, nucleophile isotope effects ranging from 1.12 to 0.93 have been measured for early and very late (essentially stepwise with formation of a phosphorane) mechanisms for nucleophilic attack[32]. Thus, determining both the leaving group and nucleophile isotope effects can therefore provide information about the general region of the MOJ diagram the TS resides in. Non-bridging oxygen KIEs ($^{18}k_{\text{NB}}$) as secondary isotope effects tend to be quite small, but can provide information about whether the TS lies on the associative or dissociative half of the MOJ diagram[33]. Because the non-bridging oxygens are not involved in the reaction coordinate, they are dominated by the TDF. An associative TS should lead to a decrease in bonding to the non-bridging oxygen atoms, and therefore a normal KIE. A dissociative TS should result in an increase in bond order to the non-bridging oxygen atoms, and therefore an inverse $^{18}k_{\text{NB}}$.

The effect of isotopic change on an equilibrium constant is referred to as an equilibrium isotope effect (EIE). Analogous to KIEs, they are represented as $K_{\text{L}}/K_{\text{H}}$, and like KIE they can be normal or inverse depending on whether the lighter or heavier atom is favored by the forward reaction. However, because EIEs do not involve the TS, there is no contribution from reaction coordinate motion and these effects can be interpreted according to the guidelines of the kinetic TDF. If a reaction mechanism involves a “pre-equilibrium” step prior to formation of the rate limiting TS, the full EIE will manifest in the observed experimental isotope effect. Therefore, these effects also play a critical role in the interpretation of observed isotope effects. These equilibrium effects must be accounted for if a pre-equilibrium step is suspected. For phosphodiester cleavage, such pre-equilibrium steps which influence the observed isotope effects involve protonation/deprotonation of nucleophilic, non-bridging, and leaving group oxygens, and these EIE are in some cases established [28,34–36]. In fact, EIE can often provide mechanistic information. For example, with non-bridging oxygen atoms, where KIE are expected to be small, the presence of a large (inverse) observed isotope effect indicates protonation occurs prior to nucleophilic attack [37,38]. This logic has been extended to support coordination of oxygen atoms by metal ions in enzymic systems [39–41].

KIEs for model diester reactions in solution

Data from the few models systems where KIEs have been determined for the leaving group, non-bridging, and nucleophile positions help illustrate how the magnitude of these measurements reveals mechanistic detail. The phosphodiester system best characterized by KIE is alkaline cleavage of the bond to a *p*-nitrophenolate leaving group (pNPP, Figure 6) via nucleophilic attack by hydroxide [37,38]. The leaving group KIE for this reaction was only 1.0063. Since ^{18}O leaving group effects range from unity to ca. 1.07 (see above), this relatively small magnitude suggested that bond cleavage was not well advanced in the TS, placing it in the early portion of the progress coordinate of the MOJ diagram (Figure 7). However, the non-bridging KIE was slightly inverse at 0.9945. The inverse nature of this effect is inconsistent with an associative TS, where advanced bonding to the nucleophile would reduce bonding to the non-bridging oxygen atoms, resulting in a normal KIE. Thus, these two effects suggested a concerted TS that resides on the early portion of the progress coordinate and perhaps in the dissociative portion of the tightness coordinate. This interpretation was supported by determination of the nucleophile isotope effect using thymidine-5'-*p*-nitrophenyl phosphate (T-5'-pNPP) [42]. Here, the observed effect was 1.068. Nucleophile effects, as indicated above can be inverse or normal depending on the TIF and TDF contributions and can range from 1.12 – 0.93. Thus, the large magnitude of this normal isotope effect indicated that the full normal EIE contribution from deprotonation to form hydroxide (K_{OH}) contributes to the observed KIE (Figure 9). Indeed, ionic strength effects on reaction rate for hydrolysis relative to neutral

nucleophiles and the presence of an alpha effect when peroxide is the nucleophile support the conclusion that the nucleophile undergoes equilibrium deprotonation to yield hydroxide prior to attack. Even accounting for the EIE on deprotonation, the KIE (k_{BOND}) was normal at 1.027. This value indicates the TIF is dominant over the TDF, supporting an early, concerted TS.

An additional phosphodiester system with both leaving group and nucleophile isotope effects reported involves catalysis of nitrophenol displacement by a dinuclear Co^{2+} complex [43,44]. The results appear to exemplify the two step mechanism envisioned for RNA hydrolysis. The nucleophile isotope effect is both inverse and extremely large ($^{18}k_{\text{NUC}} = 0.937$) indicative of advanced bond formation to the nucleophile. Indeed, the value was interpreted to indicate that the mechanism occurs through the pentavalent intermediate found at the extreme associative end of the tightness coordinate (Figure 7). In this mechanism the $^{18}k_{\text{NUC}}$ essentially becomes reflective of the EIE on going from an O-H to the much stiffer O-P bond. A large leaving group isotope effect of 1.029 suggests a late TS for the bond cleavage step. However, this example also demonstrates the limitations of KIEs as these observed effects cannot definitively distinguish between this associative mechanism and a concerted reaction with a TS lying on the late portion of the progress coordinate. Still, the ability to restrict the TS in one of two narrow regions of the MOJ diagram demonstrates their usefulness.

The *p*-nitrophenolate leaving group has been the most popular leaving group for phosphodiester KIE studies both for technical reasons and because its reactivity allows the reaction to occur in a reasonable timeframe. However, in ribozyme catalyzed reactions the leaving group is much less reactive 3' and 5' ribose oxygens, which is likely to alter the TS charge distribution. The effects of changes in nucleophile and leaving group reactivity on observed IEs appear to be quite large, however, only a few studies have been done. One such study used a *m*-nitrobenzyl leaving group attached to the 3' hydroxyl of uridine to study the attack by the 2' hydroxyl (U-3'-mNBP, Figure 6, [45]). For the alkaline reaction, the leaving group isotope effect was 1.027. Again, the large KIE indicates advanced bond cleavage in the TS. A corresponding nucleophile isotope effect has not been measured. A stepwise mechanism with a stable phosphorane intermediate was ruled out because pseudorotation indicative of the formation of a 2',3' cyclic phosphorane intermediate was not observed. Therefore, the leaving group isotope effect was interpreted to indicate a late, concerted TS.

Recently, Hengge and colleagues examined the nucleophile and leaving group isotope effects for base catalyzed reactions of hydroxypropyl-*p*-nitrophenol phosphate (HP-3'-pNPP) in which nucleophilic attack by the propyl hydroxyl mimics the intramolecular 2'-O-transphosphorylation reaction of RNA [46]. Here, the analog of the 3'O has been replaced with sulfur, however, the results provide insight into the mechanism of such intramolecular transphosphorylation reactions. An observed $^{18}k_{\text{NUC}}$ of 1.12 is assumed to include a large normal contribution from equilibrium deprotonation to yield the more reactive oxyanion. This effect for an alcohol is estimated at 1.015, and thus the intrinsic effect on bond formation is still very large and normal indicative of a very early TS with respect to bond formation. The $^{18}k_{\text{LG}}$ was determined to be 1.012, and thus leaving group departure occurs in the rate limiting step of the reaction which is presumed to be concerted (Figure 7). Compared to the results for displacement of the nitrophenol leaving group by intermolecular attack by hydroxide, the significantly greater value for $^{18}k_{\text{LG}}$ (1.012 versus 1.003) indicates a TS that is later with respect to bond cleavage.

In sum, even for these relatively few systems a range of KIEs are observed with significant differences detected for inter versus intramolecular nucleophilic attack and for diesters with different leaving group relativities. Additional quantitative analyses of KIEs as a function of nucleophile and leaving group pKa will be necessary for interpreting potential effects active site interactions in enzyme catalyzed reactions. Also, a more comprehensive understanding of

the equilibrium EIEs on ribose hydroxyl protonation will be necessary to interpret the potential effects of proton transfer on observed KIEs. Nonetheless, there is potential for gaining significant insight already if determinations for ribozyme-catalyzed reactions can be made.

Challenges for Application of KIE Analyses to Ribozyme Systems

Synthesis of isotopically labeled nucleotides for incorporation into RNA substrates

In addition to understanding how to interpret the magnitude of IEs in terms of TS structure there are two experimental challenges that must be overcome to apply this approach to ribozyme catalysis. First, nucleoside monomers containing site-specific enrichment of O isotopes at the nucleophile, leaving group and non-bridging oxygen positions must be synthesized. For Small Ribozymes catalyzing 2'-O-transphosphorylation (see Figure 1) nucleosides enriched with ^{18}O at the 5'O and 2'O positions are necessary to measure $^{18}k_{\text{LG}}$ and $^{18}k_{\text{NUC}}$, respectively. In the intermolecular reactions catalyzed by Large ribozymes, the leaving group is always the 3'O and 3'- ^{18}O modified nucleotides are therefore necessary for probing leaving group effects. For the Group I intron, which self-splices by an overall two-step mechanism involving two subsequent transesterification reactions, the nucleophile is the 3'O of a guanosine nucleoside co-substrate, whereas in the second step the nucleophile is the 3'O that served as a leaving group in the first transesterification reaction. The Group II intron uses a similar two step mechanism, however, the nucleophile for the first step is the 2'OH of an adenosine residue located within the intron sequence. As indicated above, the nucleophile for the hydrolysis reaction catalyzed by RNase P comes from the solvent, water. Both Group I and Group II introns will catalyze hydrolysis as well, and variants that react primarily via hydrolysis are known (e.g. [47,48]).

The syntheses of isotopically enriched nucleosides using several different methods have been reported, but can be limited in terms of nucleobase identity, yield and degree of isotopic enrichment. However, there are recent advances that should allow all of the reacting atoms for ribozyme catalyzed reactions to be probed. The 3'- ^{18}O and 2'- ^{18}O derivatives of uridine and adenosine were made previously by acid catalyzed exchange into protected 3'-ketonucleoside derivatives followed by reduction[49]. However, for the reaction at C3' both ribose and xylose are formed and separation of the appropriate ribose epimer is necessary. An alternative approach has been to begin with nucleotides containing the inverted configurations at the 2'-C or 3'-C positions and modify them into good leaving groups which are subsequently replaced by using ^{18}O nucleophiles [50]. Zhong and Strobel recently reported an improved synthesis of 3'- ^{18}O adenosine using this approach as well as nucleophilic opening of a 2'3' adenosine epoxide with significantly increased regioselectivity [51]. For modification of the 2' positions of pyrimidines the hydrolysis of 2,2' and 2,3'-anhydronucleosides is a highly viable approach. However, nucleophilic attack can occur at either the 2' position in the sugar ring yielding ribose, or the 2 position of the pyrimidine base giving the arabinose epimer. Unfortunately, simple aqueous hydrolysis yields overwhelmingly the arabinose product, however, Dai et al. solved this problem by noting that the ribose product is favored by nucleophiles that are more electronegative successfully using ^{18}O -benzoic acid to generate 2'- ^{18}O -uridine with high regioselectivity [52].

The degree of enrichment for these methods can be quite high (80–90%), however, enrichment need not be to the level of isotopic purity since KIE measurements are generally done by the competitive method [10]. Determining KIEs by the competitive method involves measuring the mass ratios of a near 50/50 mixture of isotopomers at different degrees of reaction. As the reaction proceeds, the first few percent of product will become enriched in the faster reacting isotope proportional to the magnitude of the rate difference. As the reaction goes to completion the final ratio in the product will necessarily match that of the precursor. The basic procedure, therefore, is to measure isotope ratios in the product at low and complete conversion, or the

substrate at the start of the reaction and the residual substrate after partial reaction. The fraction reacted and the isotope ratio of the two samples is used to compute the isotope effect.

Advances in determination of isotopic ratios by whole molecule mass spectrometry

These measurements require the ability to determine isotope ratios with precisions better than 1%, and this degree of performance is typically achieved using isotope ratio mass spectrometry (IRMS) as described above, or scintillation counting of radioactive isotopes. These methods are highly useful, but both possess inherent limitations that restrict their application to catalytic RNAs. IRMS can analyze only small, nonpolar gasses such as CO₂, N₂, and H₂; thus, this technique can be used only when the atom of interest can be quantitatively converted to one of these gasses. Significant amounts (micro- to millimoles) of material are required for IRMS, however, the high precision permits the experiment to be done in favorable cases by measuring changes from natural abundance. Scintillation counting requires substantial double-labeling schemes involving specific isotopic pairs (usually ³H and ¹⁴C), again limiting the molecules that can be analyzed. The use of ³²P/³³P was reported by Unrau and Bartel to determine the IE for nucleoside transfer reaction catalyzed by a ribozyme derived from *in vitro* selection to achieve precisions of ca. 1–2% [53]. The ease of incorporating radioactive phosphates into RNA by enzymatic transfer makes this a potential rapid way to assess KIEs of relatively large magnitude.

One alternative to these methods highly applicable to ribozymes is whole molecule mass spectrometry. Relatively gentle ionization methods such as electrospray ionization (ESI) and matrix-assisted laser desorption ionization (MALDI) coupled with quadrupole (Q-MS) and time-of-flight MS (TOF-MS) make possible the analysis of isotope ratios for numerous biologically relevant organic molecules with molecular masses in excess of 500 Da (ref). However, sources of error in Q-MS include noise (from both the ion source and the detector), background, intensity fluctuations, and the inability to capture the entire ion current arising from individual isotopologues. Some of these effects can be minimized by working with isotope ratios near unity, utilizing background subtraction and/or injecting analyte by continuous direct infusion [54]. The m/z data encompassing the isotopic envelope are fit to an equation describing a series of equally spaced and identically shaped peaks (Figure 8) [41,42]. The analysis protocol can also be applied to quadrupole time-of-flight tandem mass spectrometry. Here, the ion of interest is selected by Q-MS then fragmented, and the resultant ions are analyzed by TOF-MS. This operation results in dramatic improvements in signal to noise, and as the TOF detector intrinsically collects a range of masses, the output data is ideal for quantitative analysis by peak fitting. An example of the primary tandem Q/TOF-MS/MS results are shown in Figure 8B. The ability to measure isotope ratios in nucleotides with high precision and sensitivity combined with the capability to synthesize RNA oligonucleotides with site-specific isotopic enrichments permit a broad range of enzymes, including ribozymes to be subject to high resolution mechanistic analyses.

One additional consideration also exists for any KIE determination for enzyme systems. KIE only probe the rate limiting step of a chemical reaction. In solution, this step almost always involves bond fission and/or formation involving the atoms in the reaction coordinate. However, enzymatic catalysis introduces numerous steps into the reaction that can be rate-limiting and do not involve bond changes in the reaction coordinate [10,26,55]. When such “non-chemical” steps are limiting, the enzyme is said to exhibit a “commitment to catalysis.” As an example, if an enzyme has a high affinity for the substrate, the chemical transformation will nearly always take place rather than substrate dissociation. Thus, the enzyme-substrate complex is committed to catalysis upon substrate binding. In this case, the commitment is termed an external commitment. However, the commitment can also occur in a conformational change of an enzyme-substrate complex which occurs after binding, but prior to the chemical

step. In these cases, the commitment is termed internal. The presence of an external commitment can be probed by pulse-chase experiments, but internal commitments can be more problematic. A more extensive treatment of commitments can be found in the reviews of enzymatic isotope effects given above.

Initial Ribozyme and Model Reaction Studies

A key feature of the mechanisms of large ribozymes, and indeed numerous phosphodiesterases is the activation of nucleophilic attack by metal ion coordination. However, probing directly whether the nucleophilic water is coordinated to a metal ion in the enzyme-catalyzed TS is difficult. For the assumed concerted mechanisms of large ribozymes, a normal $^{18}k_{\text{NUC}}$ is anticipated based on the value observed for the displacement of nitrophenol by hydroxide attack [42]. However, a key question is- What is the effect of the proposed direct coordination of the nucleophilic water by Mg^{2+} in the two metal ion model? A possible model for active site metal ion interactions in ribozymes is the catalysis of TMP-PNP hydrolysis by Mg^{2+} in solution [41]. Inclusion of Mg^{2+} increases the hydrolysis rate in part by lowering the pK_a of coordinated water molecules, thereby increasing the concentration of the lyate hydroxide. However, an additional *ca.* 100 fold greater extent of catalysis of TMP-PNP hydrolysis by Mg^{2+} is observed beyond the 100-fold expected from increasing the concentration of hydroxide by lowering pK_a . Simultaneous interaction of the metal ion with the nucleophile and phosphodiester is a likely mechanism for this additional catalysis, analogous to observation of metal ion catalysis of phosphomonoesters (REF). Interestingly, for the Mg^{2+} -catalyzed TMP-PNP hydrolysis reaction there is a significant decrease in the observed $^{18}k_{\text{NUC}}$ to 1.027 from 1.063 before accounting for any effect from deprotonation of the nucleophile. This result demonstrates a significant increase in bonding “stiffness” to the nucleophile in the TS relative to the TS in the absence of Mg^{2+} [41]. A portion of this increase in bond “stiffness” could come from coordination of the nucleophilic OH- (Figure 9). Indeed, the equilibrium isotope effect on metal ion coordination of water ($^{18}K_{\text{COORD}}$) is 0.98 [56], and could easily account for much of the difference in the $^{18}k_{\text{NUC}}$ for alkaline hydrolysis of TMP-PNP in the presence versus the absence of Mg^{2+} .

Like other large ribozymes the RNA hydrolysis reaction catalyzed by P RNA is thought to involve use active site metal ions based on the observation that rate enhancement is decreased dramatically by thio substitution of the nonbridging oxygens and 3' O [57,58]. For P RNA catalysis the magnitude of $^{18}k_{\text{NUC}}$ is normal and relatively large but less than that observed for hydroxide attack on TMP-PNP (1.027). Several factors could account for this apparently “stiffer” bonding environment for ribozyme catalyzed phosphodiester bond hydrolysis compared to the solution reaction including an enzyme commitment to catalysis or metal ion coordination to nucleophile as implied by the results from TMP-PNP hydrolysis in the presence of Mg^{2+} . Enzyme pulse chase studies showed that the observed commitment for the P RNA reaction was low. Also change in the rate of ribozyme reaction by increasing pH resulted in only a small change in the observed $^{18}k_{\text{NUC}}$, indicating that isotopic enrichment occurs at the chemical step. The most attractive possibility consistent with the proposed catalytic mechanism is that the additional stiffness in the TS of the ribozyme reaction comes from coordination to an active site metal ion as proposed for the solution hydrolysis of TMP-PNP.

Future Directions

Looking forward, intramolecular 2'-O transphosphorylation reaction catalyzed by small ribozymes is also mechanistically complex and KIE analysis is likely to provide important new detail for this class of reactions as well. Initial results for base catalyzed RNA hydrolysis indicate a transition state consistent with previous KIE results using U-3'-mNB (Harris, Dai, Piccirilli and Anderson, unpublished). For such intramolecular phosphoryl transfer reactions

understanding whether a phosphorane form will clearly be important. If such an intermediate forms for the ribozyme reaction it raises the possibility that an additional active site interaction occurs to protonate one of the non-bridging oxygens. If the mechanism has an early TS with respect to nucleophile bond formation, then a normal $^{18}k_{\text{NUC}}$ would be predicted. By analogy to the model reaction of CoIII complex characterized by Hengge (see above) a completely stepwise mechanism shows a significantly inverse $^{18}k_{\text{NUC}}$. Thus, observation of such a strongly inverse $^{18}k_{\text{NUC}}$ would provide a clue as to whether an intermediate forms.

In particular the magnitude of KIEs for the reactions catalyzed by small ribozymes could be important for characterizing the extent of proton transfer in the TS and thus provide better understanding models of acid-base catalysis. As detailed above, protonation and deprotonation will influence the magnitude of observed leaving group and nucleophile KIEs, respectively. Pre-equilibrium protonation/deprotonation will result in the greatest contribution up a maximum limited by EIE for proton transfer. While the EIE for deprotonation of water to yield OH⁻ is known (1.04) the effect for proton transfer to alcohols like the 2'OH has not been measured directly and determining this value is necessary for interpreting KIEs for 2'-O-transphosphorylation. Additionally, Anderson and colleagues showed that the strength of the H-bond donation by alcohols is reflected in the carbon-hydrogen bond of the H-C-O-H functional group[59,60]. The change in ionization for the nucleophile and leaving group in small ribozymes could in principle be monitored by determining the effect of a secondary deuterium isotope effect on either C2' or C5', respectively. While synthetic and experimental obstacles remain, there is clearly impetus for further analysis of both primary and secondary KIEs in ribozymes.

Based on the extensive studies of phosphoryl transfer reactions in solution and both ribozyme and protein enzymology to date, the fundamental questions to be addressed in characterizing ribozyme catalytic function include the following. Are mechanisms concerted or stepwise? Do the nucleophile and leaving group undergo changes in protonation by pre-equilibration or are protons 'in flight' in the TS? Does one (probably not more) of the non-bridging oxygens become protonated during the reaction? Are metal ions in the active site acting by facilitating proton transfer via their coordinated waters, acting as Lewis acids to offset charge, or acting electrophilically via direct coordination to the phosphate oxygens? The chemical interactions and transformations implied by these questions result in dramatic differences in the vibrational properties of the reacting atoms in the TS. Thus, characterizing values for KIEs on nucleophile, leaving group and non-bridging oxygens for ribozyme catalyzed reactions are of immediate value. However, the magnitude of the observed KIE will be sensitive to all of the vibrational modes that are different between the ground state and the TS. An example of this is the nucleophile effect on diester hydrolysis which is likely to contain contributions from deprotonation, desolvation and potentially metal ion coordination in addition to the effect on bond formation as described above. While important information on mechanism such as whether the reaction is concerted or stepwise can likely be gained in the immediate term, interpreting KIEs in a more detailed manner will require additional synergy between parallel results from reactions of model compounds in solution together with coordinated physical organic analysis together with high level computational simulations.

Acknowledgments

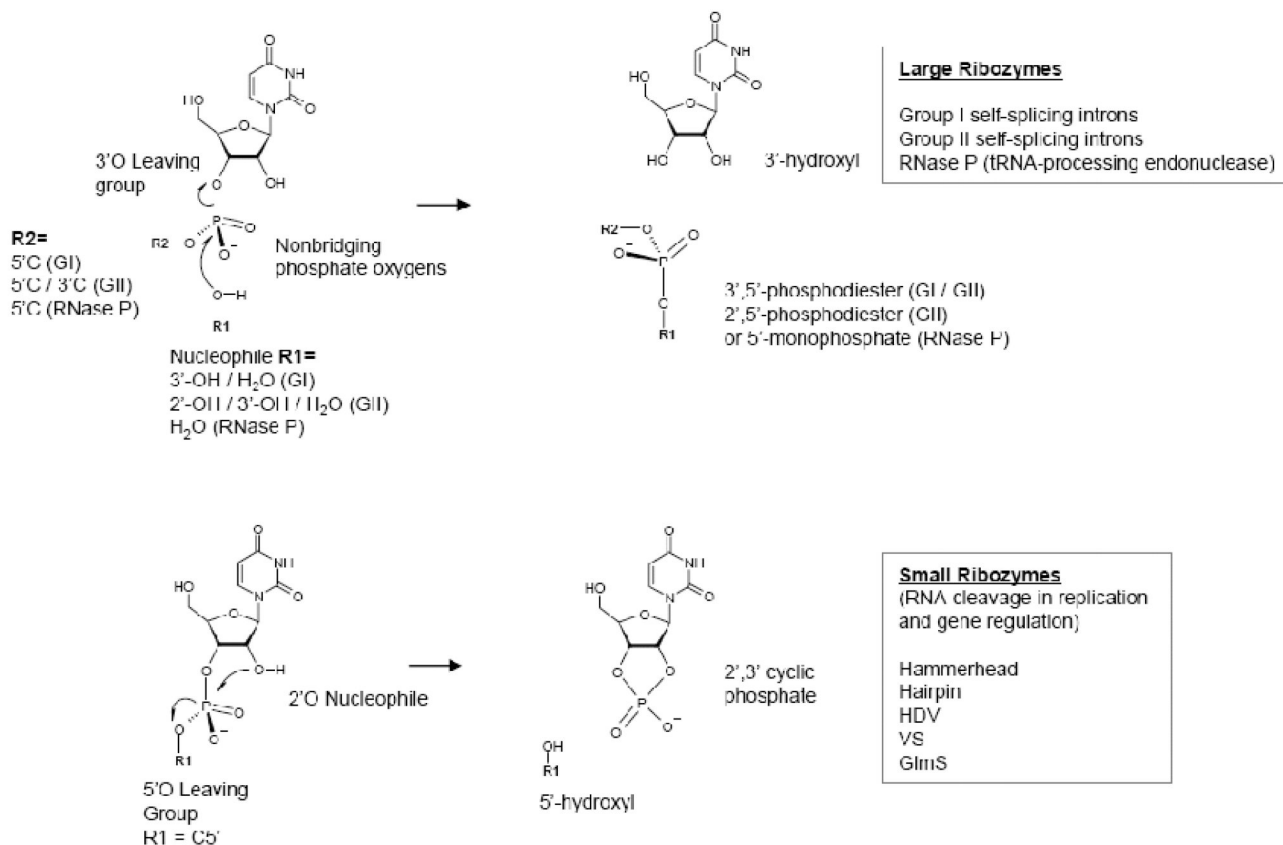
We are particularly indebted to Drs. Joe Piccirilli and Vernon Anderson for support and advice on execution and interpretation of KIE experiments as well as insightful comments on the manuscript. We also sincerely thank Drs. Phil Bevilacqua, Barbara Golden, Eric Christian for helpful discussions and comments. Limitations of space preclude a complete reference list for foundational studies of RNA structure, enzyme catalysis, and phosphoryl transfer chemistry. Accordingly we beg the indulgence of colleagues who are not more thoroughly acknowledged.

References

1. Weinger JS, Strobel SA. Participation of the tRNA A76 hydroxyl groups throughout translation. *Biochemistry* 2006;45:5939–5948. [PubMed: 16681365]
2. Steitz TA. A structural understanding of the dynamic ribosome machine. *Nat Rev Mol Cell Biol* 2008;9:242–253. [PubMed: 18292779]
3. Rodnina MV, Beringer M, Wintermeyer W. Mechanism of peptide bond formation on the ribosome. *Q Rev Biophys* 2006;39:203–225. [PubMed: 16893477]
4. Doudna JA, Lorsch JR. Ribozyme catalysis: not different, just worse. *Nat Struct Mol Biol* 2005;12:395–402. [PubMed: 15870731]
5. Fedor MJ, Williamson JR. The catalytic diversity of RNAs. *Nat Rev Mol Cell Biol* 2005;6:399–412. [PubMed: 15956979]
6. Lilley DM. Structure, folding and mechanisms of ribozymes. *Curr Opin Struct Biol* 2005;15:313–323. [PubMed: 15919196]
7. Sigel RK, Pyle AM. Alternative roles for metal ions in enzyme catalysis and the implications for ribozyme chemistry. *Chem Rev* 2007;107:97–113. [PubMed: 17212472]
8. Strobel SA, Cochrane JC. RNA catalysis: ribozymes, ribosomes, and riboswitches. *Curr Opin Chem Biol* 2007;11:636–643. [PubMed: 17981494]
9. Cleland WW, Hengge AC. Enzymatic mechanisms of phosphate and sulfate transfer. *Chem Rev* 2006;106:3252–3278. [PubMed: 16895327]
10. Cleland WW. The use of isotope effects to determine enzyme mechanisms. *Arch Biochem Biophys* 2005;433:2–12. [PubMed: 15581561]
11. Schramm VL. Enzymatic transition state theory and transition state analogue design. *J Biol Chem* 2007;282:28297–28300. [PubMed: 17690091]
12. Jencks WP. Binding energy, specificity, and enzymic catalysis: the circe effect. *Adv Enzymol Relat Areas Mol Biol* 1975;43:219–410. [PubMed: 892]
13. Walsh, C. *Enzymatic Reaction Mechanisms*. San Francisco: W. H. Freeman and Company; 1979.
14. Jencks WP. General acid-base catalysis of complex reactions in water. *Chem Rev* 1972;72:705–718.
15. O'Ferrel MRA. Relationships between E2 and E1 cB mechanisms of beta-elimination. *J Chem Soc B* 1970;1970:274–277.
16. Zalatan JG, Herschlag D. Alkaline phosphatase mono- and diesterase reactions: comparative transition state analysis. *J Am Chem Soc* 2006;128:1293–1303. [PubMed: 16433548]
17. Kirby AJ, Younas M. The reactivity of phosphate esters. Reactions of diesters with nucleophiles. *J Chem Soc B* 1970;1970:1165–1172.
18. Ye JD, Barth CD, Anjaneyulu PS, Tuschl T, Piccirilli JA. Reactions of phosphate and phosphorothiolate diesters with nucleophiles: comparison of transition state structures. *Org Biomol Chem* 2007;5:2491–2497. [PubMed: 17637971]
19. Leffler J. Parameters for the Description of Transition States. *Science* 1953;117:340–341. [PubMed: 17741025]
20. Davis AM, Hall AD, Williams A. Charge description of base-catalyzed alcoholysis of aryl phosphodiester: A ribonuclease model. *J Am Chem Soc* 1988;110:5105–5108.
21. Kosonen M, Youseti-Salakdeh E, Strömberg R, Lönnberg H. Mutual isomerization of uridine 2- and 3-alkylphosphates and cleavage to a 2,3-cyclic phosphate: the effect of the alkyl group on the hydronium- and hydroxide-ion-catalyzed reactions. *J Chem Soc Perk Trans 2* 1997:2661–2666.
22. Lönnberg H, Stromberg R, Williams A. Compelling evidence for a stepwise mechanism of the alkaline cyclisation of uridine 3'-phosphate esters. *Org Biomol Chem* 2004;2:2165–2167. [PubMed: 15280948]
23. Bigeleisen J, Wolfsberg M. Theoretical and experimental aspects of isotope effects in chemical kinetics. *Adv. Chem. Phys* 1958;1:15–76.
24. Schramm VL. Enzymatic transition states and transition state analog design. *Annu Rev Biochem* 1998;67:693–720. [PubMed: 9759501]
25. Cleland WW. The use of isotope effects to determine transition-state structure for enzymic reactions. *Methods Enzymol* 1982;87:625–641. [PubMed: 7176928]

26. Cleland WW. Isotope effects: determination of enzyme transition state structure. *Methods in Enzymology* 1995;249:341–373. [PubMed: 7791618]
27. Hengge AC. Isotope effects in the study of enzymatic phosphoryl transfer reactions. *FEBS Lett* 2001;501:99–102. [PubMed: 11470264]
28. Hengge AC. Isotope effects in the study of phosphoryl and sulfonyl transfer reactions. *Acc Chem Res* 2002;35:105–112. [PubMed: 11851388]
29. Jencks, WP. *Catalysis in Chemistry and Enzymology* (McGraw-Hill Series in Advanced Chemistry). 1969.
30. Buddenbaum WE, Shriner VJ. ^{13}C kinetic isotope effects and reaction coordinate motions in transition states for $\text{S}_{\text{N}}2$ displacement reactions. *Canadian Journal of Chemistry* 1976;54:1146–1161.
31. Paneth P, O'Leary MH. Nitrogen and deuterium isotope effects on the quarternization of N,N-dimethyl-p-toluidine. *J Am Chem Soc* 1991;113:1691–1693.
32. Hengge A, Onyido I. Physical Organic Perspectives on Phospho Group Transfer From Phosphates and Phosphinates. *Curr Org Chem* 2005;9:61–74.
33. Cleland WW, Hengge AC. Mechanisms of phosphoryl and acyl transfer. *FASEB Journal* 1995;9:1585–1594. [PubMed: 8529838]
34. Hengge AC, Hess RA. Concerted or stepwise mechanisms for acyl transfer reactions of p-nitrophenyl acetate? transition state structures from isotope effects. *Journal of the American Chemical Society* 1994;116:11256–11263.
35. Knight WB, Weiss PM, Cleland WW. Determination of equilibrium ^{18}O isotope effects on the deprotonation of phosphate and phosphate esters and the anomeric effect on deprotonation of glucose-6-phosphate. *Journal of the American Chemical Society* 1986;108:2759–2761.
36. Green M, Taube H. Isotopic fractionation in the $\text{OH}-\text{H}_2\text{O}$ exchange reaction. *J. Phys. Chem* 1963;67:1565–1566.
37. Hengge AC, Cleland WW. Phosphoryl-transfer reactions of phosphodiester: characterization of transition states by heavy-atom isotope effects. *J Am Chel Soc* 1991;vol 113:5835–5841.
38. Hengge AC, Aleksandra TE, Cleland WW. Studies of transition-state structures of phosphoryl transfer reactions of phosphodiester of p-nitrophenol. *J Am Chem Soc* 1995;117:5919–5926.
39. Zalatan JG, Catrina I, Mitchell R, Grzyska PK, O'Brien PJ, Herschlag D, Hengge AC. Kinetic isotope effects for alkaline phosphatase reactions: implications for the role of active-site metal ions in catalysis. *J Am Chem Soc* 2007;129:9789–9798. [PubMed: 17630738]
40. Catrina I, O'Brien PJ, Purcell J, Nikolic-Hughes I, Zalatan JG, Hengge AC, Herschlag D. Probing the origin of the compromised catalysis of *E. coli* alkaline phosphatase in its promiscuous sulfatase reaction. *J Am Chem Soc* 2007;129:5760–5765. [PubMed: 17411045]
41. Cassano AG, Anderson VE, Harris ME. Analysis of Solvent Nucleophile Isotope Effects: Evidence for Concerted Mechanisms and Nucleophilic Activation by Metal Coordination in Nonenzymatic and Ribozyme-Catalyzed Phosphodiester Hydrolysis. *Biochemistry* 2004;43:10547–10559. [PubMed: 15301552]
42. Cassano AG, Anderson VE, Harris ME. Evidence for direct attack by hydroxide in phosphodiester hydrolysis. *Journal of the American Chemical Society* 2002;124:10964–10965. [PubMed: 12224928]
43. Humphry T, Forconi M, Williams NH, Hengge AC. An altered mechanism of hydrolysis for a metal-complexed phosphate diester. *J Am Chem Soc* 2002;124:14860–14861. [PubMed: 12475323]
44. Humphry T, Forconi M, Williams NH, Hengge AC. Altered mechanisms of reactions of phosphate esters bridging a dinuclear metal center. *J Am Chem Soc* 2004;126:11864–11869. [PubMed: 15382921]
45. Gerratana B, Sowa GA, Cleland WW. Characterization of the transition state structures and mechanisms for the isomerization and cleavage reactions of 3'-m-nitrobenzyl phosphate. *J Am Chem Soc* 2000;122:12615–12621.
46. Iyer S, Hengge AC. The Effects of Sulfur Substitution for the Nucleophile and Bridging Oxygen Atoms in Reactions of Hydroxyalkyl Phosphate Esters. *J Org Chem* 2008;6:6.
47. Jabri E, Aigner S, Cech TR. Kinetic and secondary structure analysis of Naegleria andersoni GIR1, a group I ribozyme whose putative biological function is site-specific hydrolysis. *Biochemistry* 1997;36:16345–16354. [PubMed: 9405070]

48. Podar M, Chu VT, Pyle AM, Perlman PS. Group II intron splicing in vivo by first-step hydrolysis. *Nature* 1998;391:915–918. [PubMed: 9495347]
49. Wnuk SF, Chowdhury SM, Garcia PI Jr, Robins MJ. Stereodefined synthesis of O3'-labeled uracil nucleosides. 3'-[(17)O]-2'-Azido-2'-deoxyuridine 5'-diphosphate as a probe for the mechanism of inactivation of ribonucleotide reductases. *J Org Chem* 2002;67:1816–1819. [PubMed: 11895397]
50. Jiang CS, R J, Baker DC. Oxygen-18-labeled adenosine and 9-(b-D-arabinofuranosyl)adenine (ARA-A): synthesis, mass spectrometry, and studies of oxygen-18-induced carbon-13 NMR chemical shifts. *Nucleosides Nucleotides* 1988;7:271–294.
51. Zhong M, Strobel SA. Synthesis of isotopically labeled p-site substrates for the ribosomal peptidyl transferase reaction. *J Org Chem* 2008;73:603–611. [PubMed: 18081346]
52. Dai Q, Frederiksen JK, Anderson VE, Harris ME, Piccirilli JA. Efficient synthesis of [2'-18O]uridine and its incorporation into oligonucleotides: a new tool for mechanistic study of nucleotidyl transfer reactions by isotope effect analysis. *J Org Chem* 2008;73:309–311. [PubMed: 18052189]
53. Unrau PJ, Bartel DP. An oxocarbenium-ion intermediate of a ribozyme reaction indicated by kinetic isotope effects. *Proc Natl Acad Sci U S A* 2003;100:15393–15397. [PubMed: 14668444]
54. Cassano AG, Wang B, Anderson DR, Previs S, Harris ME, Anderson VE. Inaccuracies in selected ion monitoring determination of isotope ratios obviated by profile acquisition: nucleotide 18O/16O measurements. *Anal Biochem* 2007;367:28–39. [PubMed: 17560863]
55. Cleland WW. Use of isotope effects to elucidate enzyme mechanisms. *CRC Crit Rev Biochem* 1982;13:385–428. [PubMed: 6759038]
56. Feder HM, Taube H. Ionic hydration: an isotopic fractionation technique. *J. Chem. Phys* 1952;20:1335–1336.
57. Warnecke JM, Sontheimer EJ, Piccirilli JA, Hartmann RK. Active site constraints in the hydrolysis reaction catalyzed by bacterial RNase P: analysis of precursor tRNAs with a single 3'-S-phosphorothioate internucleotide linkage. *Nucleic Acids Res* 2000;28:720–727. [PubMed: 10637323]
58. Warnecke JM, Furste JP, Hardt WD, Erdmann VA, Hartmann RK. Ribonuclease P (RNase P) RNA is converted to a Cd(2+)-ribozyme by a single Rp-phosphorothioate modification in the precursor tRNA at the RNase P cleavage site. *Proc Natl Acad Sci U S A* 1996;93:8924–8928. [PubMed: 8799129]
59. Maiti NC, Zhu Y, Carmichael I, Serianni AS, Anderson VE. 1JCH correlates with alcohol hydrogen bond strength. *J Org Chem* 2006;71:2878–2880. [PubMed: 16555846]
60. Maiti NC, Carey PR, Anderson VE. Correlation of an alcohol's (alpha)C-D stretch with hydrogen bond strength in complexes with amines. *J Phys Chem A* 2003;107:9910–9917.

**Figure 1.**

General mechanisms of the RNA hydrolysis and transphosphorylation reactions catalyzed by Large and Small Ribozymes. **A.** Intermolecular nucleophilic attack by solvent or ribose 2' or 3' hydroxyl catalyzed by Large Ribozymes. Nucleophilic attack is by 3'OH, 2'OH or water to displace the 3'O of a phosphodiester bond in the substrate RNA yielding products containing a 3'OH and a 3',5'phosphodiester or 2'5'-phosphodiester for self-splicing Group I and Group II intron ribozymes, or a 5' phosphate in the case of the RNase P ribozyme. **B.** Intramolecular 2'-O-transphosphorylation catalyzed by Small Ribozymes. 2'OH nucleophilic attack and displacement of the 5'O leaving group generate a 2',3' cyclic phosphate and a 5' OH product.

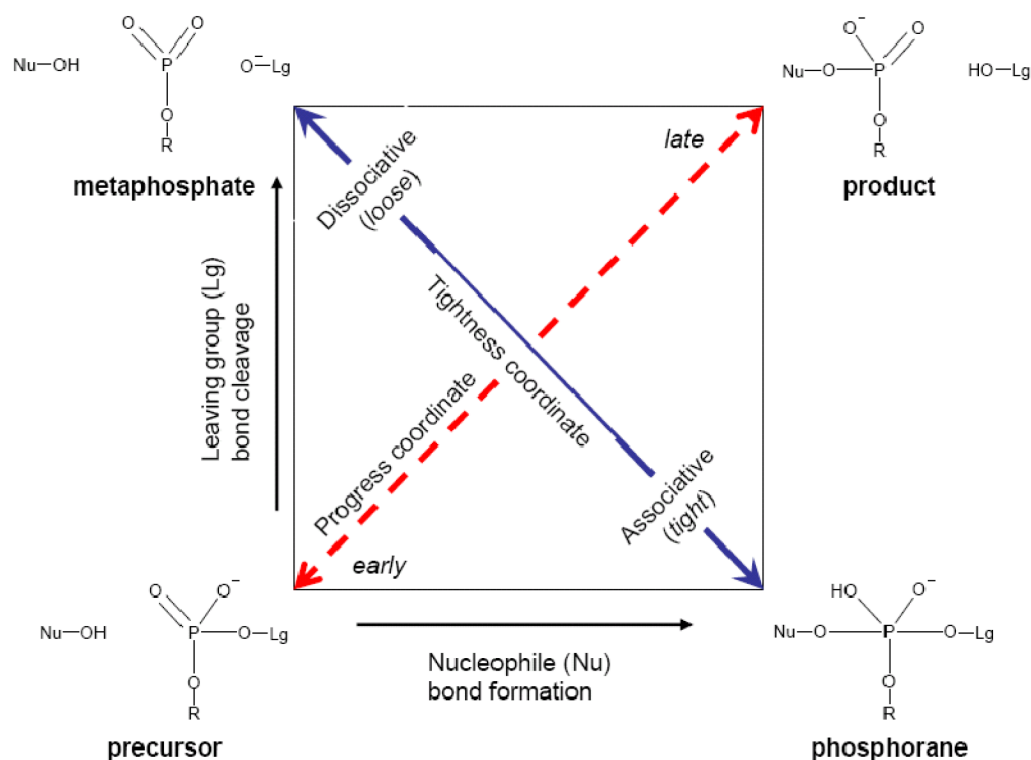


Figure 2.

A. Moore-O'Ferrel/Jencks (MOJ) diagram of the mechanistic landscape for phosphodiester addition/displacement reactions.[14,15]. The precursor phosphodiester is located at the bottom left corner of the diagram and the transferred, or hydrolyzed product is located at the upper right. The horizontal coordinate represents Nucleophile (Nu) bond formation and the vertical coordinate represents Leaving group (Lg) bond cleavage. The TS for a concerted reaction occupies a point within this landscape that is the lowest barrier along the reaction coordinate connecting the precursor and product. The diagonal “progress” coordinate describes whether the transition state is “early” or precursor-like, or “late” meaning product-like. Correspondingly, the “tightness” coordinate describes the extent to which the TS is dissociative resembling metaphosphate, or associative resembling a phosphorane. The phosphorane and metaphosphate structures at the boundaries of the tightness coordinate are located at the lower right and upper left of the diagram, respectively.

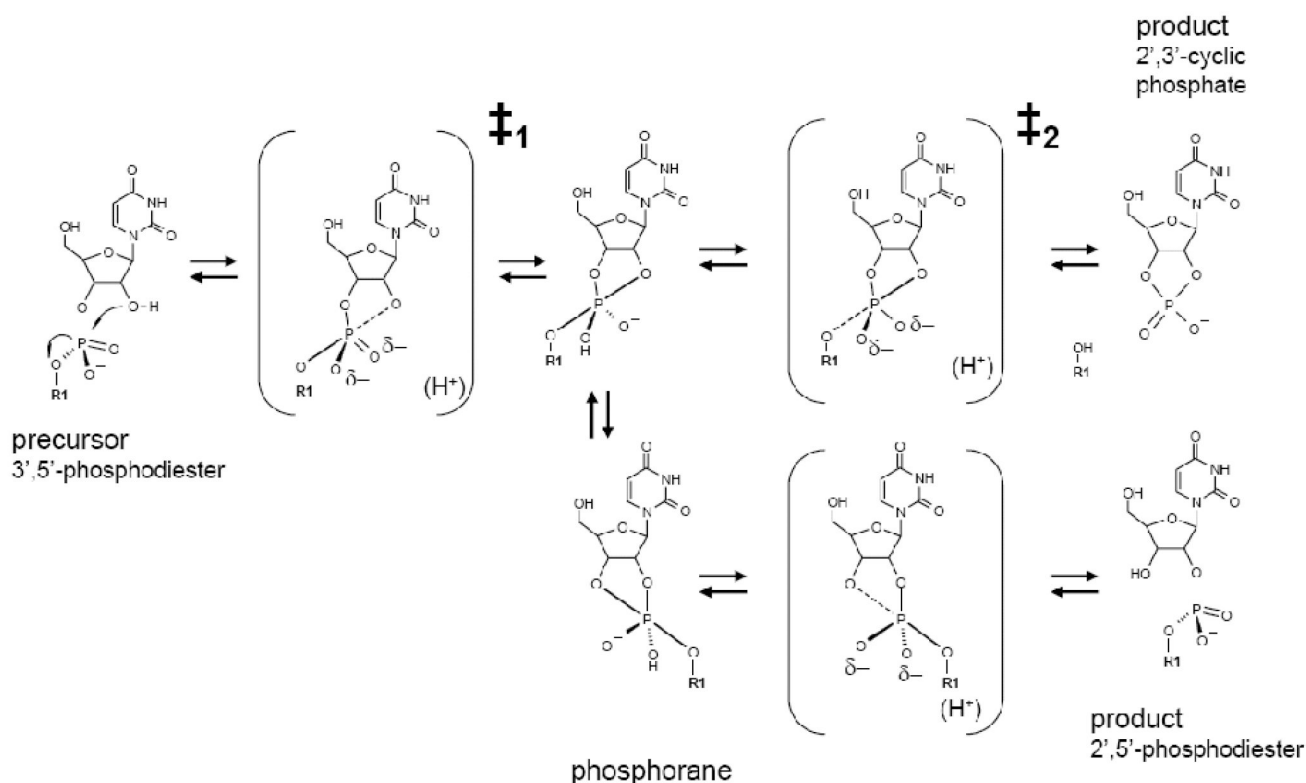


Figure 3.

Stepwise mechanisms leading to cleavage and isomerization during the neutral and acidic 2'-O-transphosphorylation reactions of RNA. Nucleophilic attack occurs in the initial step via the transition state labeled, \ddagger_1 , to form a phosphorane intermediate. Because the timing and trajectory of proton transfer is not defined for these reactions the nucleophile is depicted bearing a partial negative charge and the H^+ symbol within the brackets containing the transition state structure represents the departed of the proton from the 2'OH in either a pre-equilibrium step or in the process of being transferred in the TS. As described in the text the phosphorane intermediate can undergo rearrangement to make the 3'O a potential leaving group from this structure. Departure of the 5'O results in the 2'3'-cyclic phosphate and 5'OH products shown on top. Alternatively, pseudorotation followed by departure of the 3'O results in the formation of a 2',5'-phosphodiester product shown on the bottom. These leaving group displacement reactions from the phosphorane intermediate occur via a second transition state (\ddagger_2). As in \ddagger_1 the ambiguity regarding proton transfer is represented by the presence of the (H^+) symbol.

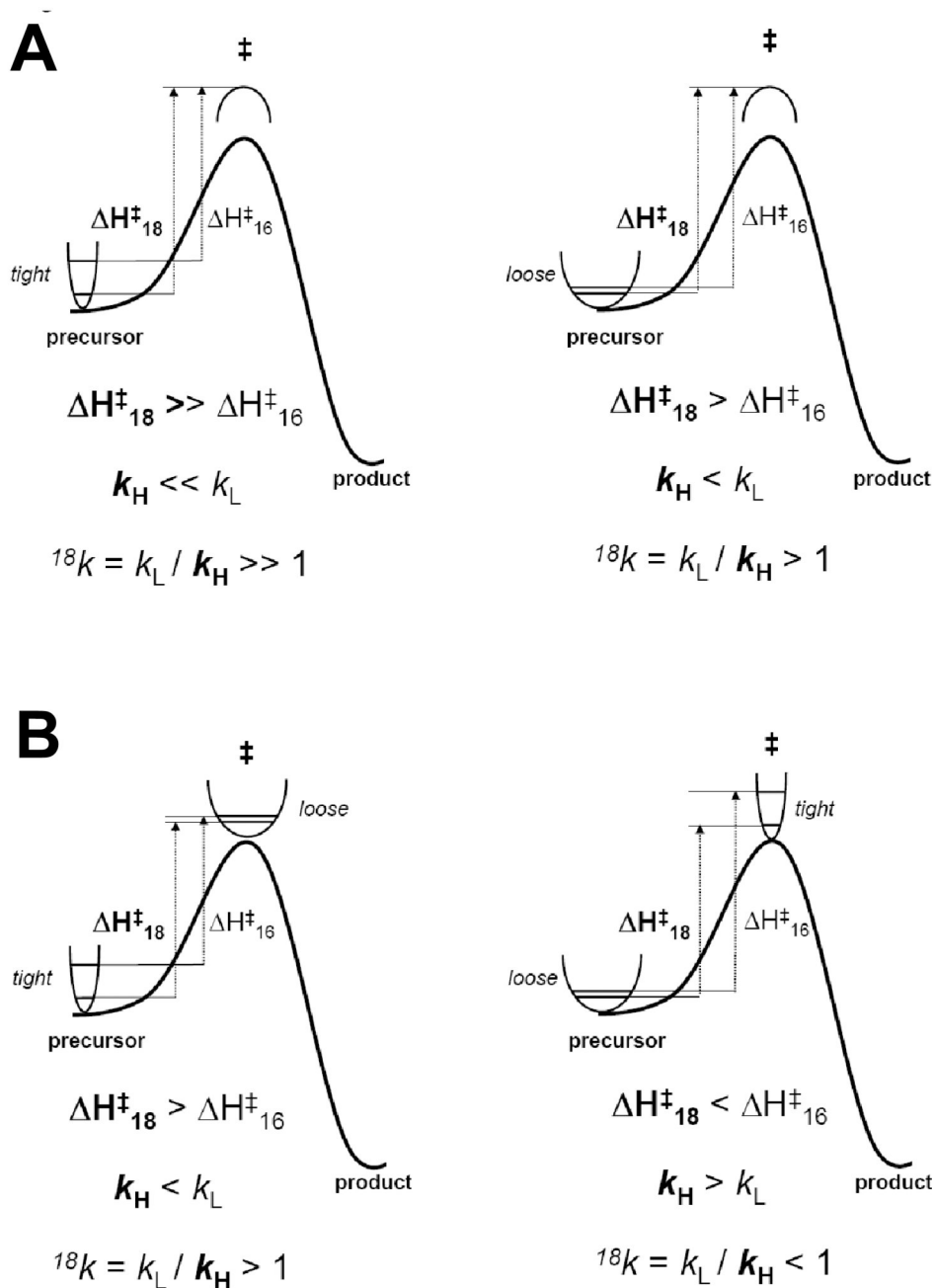


Figure 4. Reaction coordinate diagrams illustrating how changes in bond “stiffness” between the ground state and transition state result in selective enrichment of either ^{18}O or ^{16}O in the product. **A.** Representation of the contribution from the TIF. A hypothetical reaction coordinate (thick line) connects the precursor (left) and product (right) going through a single transition state (‡). This contribution arises from the frequency that is lost in the transition state that represents reaction coordinate motion. Since there is no restoring force to this vibration the barrier for the heavy and light isotopes is the same and the difference in reaction rate is due to differences in ground state zero point energies. The substrate containing the heavy isotope will have an activation energy (ΔH_{18}) is always greater than that for the lighter isotope (ΔH_{16}). As a result the rate of

reaction for the precursor substituted with the heavy isotope is less ($k_H < k_L$). This difference gives rise to a normal isotope effect that is greater than unity. **B.** Representation of the contribution from the TDF. A similar hypothetical reaction coordinate is shown as in part A. In the example on the left the vibrational environment of the substituted atom becomes less stiff (i.e. “loose”) in the transition state represented by a more broad energy well compared to the ground state of the precursor (“tight”). Because the tighter bonding environment results in a greater difference in the vibrational energy levels of the heavy and light isotopes the activation energy for the precursor containing the heavy isotope (ΔH_{18}) is greater than that for the lighter isotope (ΔH_{16}). As a result the rate of reaction for the precursor substituted with the heavy isotope is less ($k_H < k_L$). This difference gives rise to a normal isotope effect that is greater than unity. In contrast, on the right is shown a reaction coordinate in which the bonding environment of the reacting atom becomes more stiff in the transition state resulting in an inverse isotope effect that is less than unity.

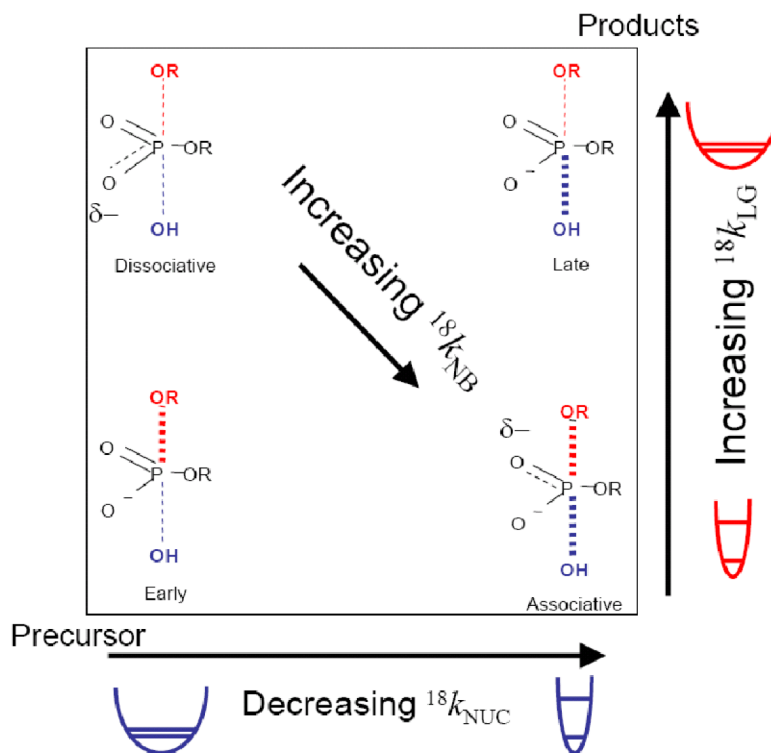
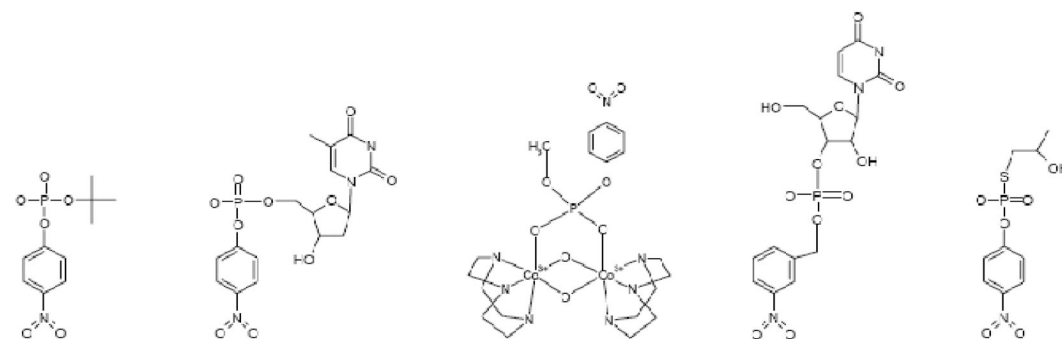


Figure 5. Relative magnitudes of $^{18}k_{\text{NUC}}$, $^{18}k_{\text{NB}}$ and $^{18}k_{\text{LG}}$ provide information on the position of the TS in the energetic landscape defined by the MOJ diagram. Loose (early) and stiff (late) bonding environments for the nucleophile are depicted in blue. Similar representations of the leaving group bonding are shown in red. The positions of the precursor and product are the same as in Figure 2



	pNPP	T-5'-pNPP	Co(III) complex	U-3'-mNBP	HP-3'-pNPP
$^{18}k_{\text{NUC}}$	nd	1.068(1.27) [42]	0.937 [43,44]	nd	1.12(1.08) [46]
$^{18}k_{\text{LG}}$	1.0063 [37,38]	nd	1.029 [43,44]	1.027 [45]	1.012 [46]

Figure 6.

Model compounds used in solution KIE analyses. pNPP, *p*-nitrophenol; T-5'-pNPP, thymidine-*p*-nitrophenol phosphate; U-3'-pNPP, uridine-3'-*p*-nitrophenol phosphate; U-3'-mNB, uridine-3'-nitrobenzyl phosphate; HP-3'-pNPP, hydroxypropyl-*p*-nitrophenol phosphate. The $^{18}k_{\text{NUC}}$ and $^{18}k_{\text{LG}}$ values determined for the base catalyze reactions of these compounds are shown. The observed nucleophile isotope effects for T-5'-pNPP and for HP-3'-pNPP corrected for equilibrium deprotonation prior to nucleophilic attack are shown in parenthesis. For T-5'-pNPP the EIE for deprotonation of water of 1.04 is used as described in the text. The EIE for deprotonation of HP-3'-pNPP is less clear and may be significantly lower than the value of 1.04 assumed here as discussed in [46].

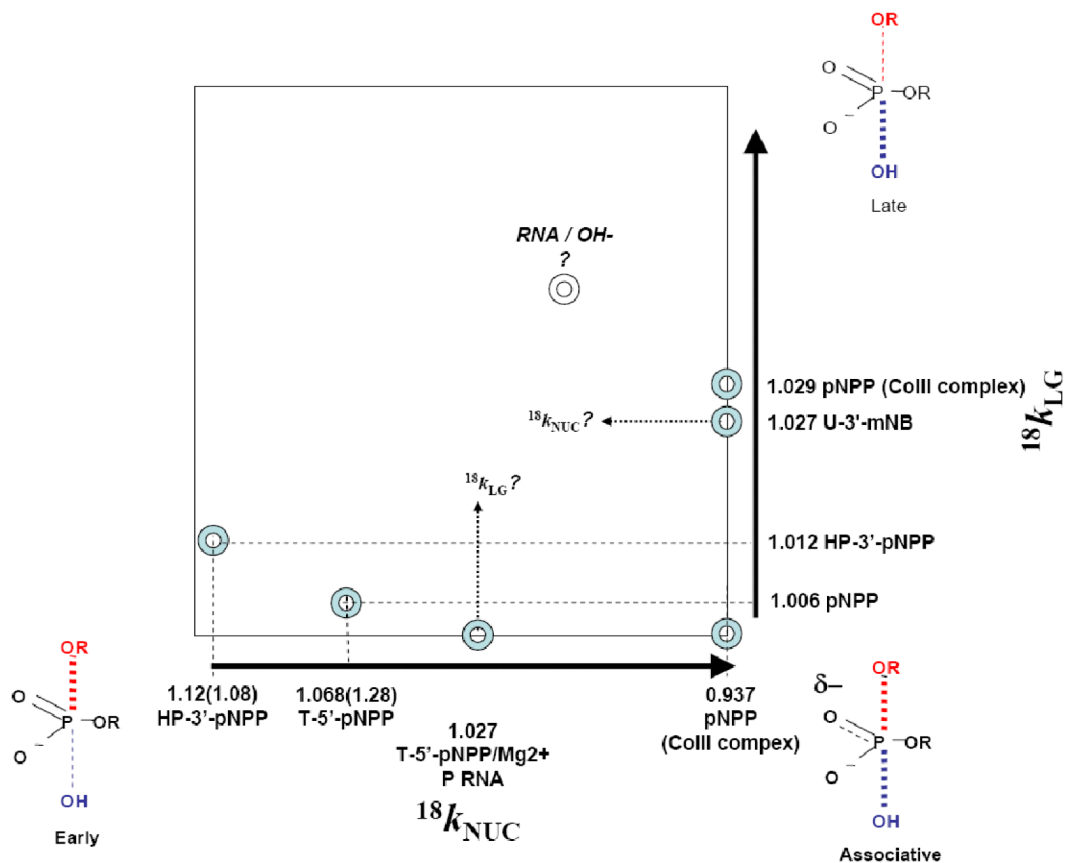


Figure 7.

Determination of mass ratios in nucleotides by ESI-Q MS and tandem ESI-Q/TOF MS/MS. **A.** An example of a mass spectrum of mass/charge (m/z) versus ion intensity for a mixture of thymidine-5'-monophosphate and 5'- ^{18}O -thymidine-5'-monophosphate ($[5\text{'-}^{18}\text{O}]\text{TMP}$) is shown. The mass spectrum was obtained by direct infusion by ESI and separation by quadrupole mass spectrometry. The individual points are the intensity data at different m/z values and the solid line is a fit of these data to a series of Gaussian peaks as described in the text. **B.** Example of results from tandem ESI-Q/TOF MS/MS analysis of natural abundance uridine-3'-monophosphate. The figure shows the product ion spectrum of 3'-UMP after selection of the parent ion by quadrupole MS followed by collision fragmentation. The resultant ribosyl phosphate ion has a mass of 211 mu. The additional peaks at $M+1$ and $M+2$ come from the presence of natural abundance deuterium and ^{18}O present in the molecule. The inset shows a blowup of the natural abundance peaks to illustrate the dramatic enhancement in signal to noise relative to ESI-Q MS.

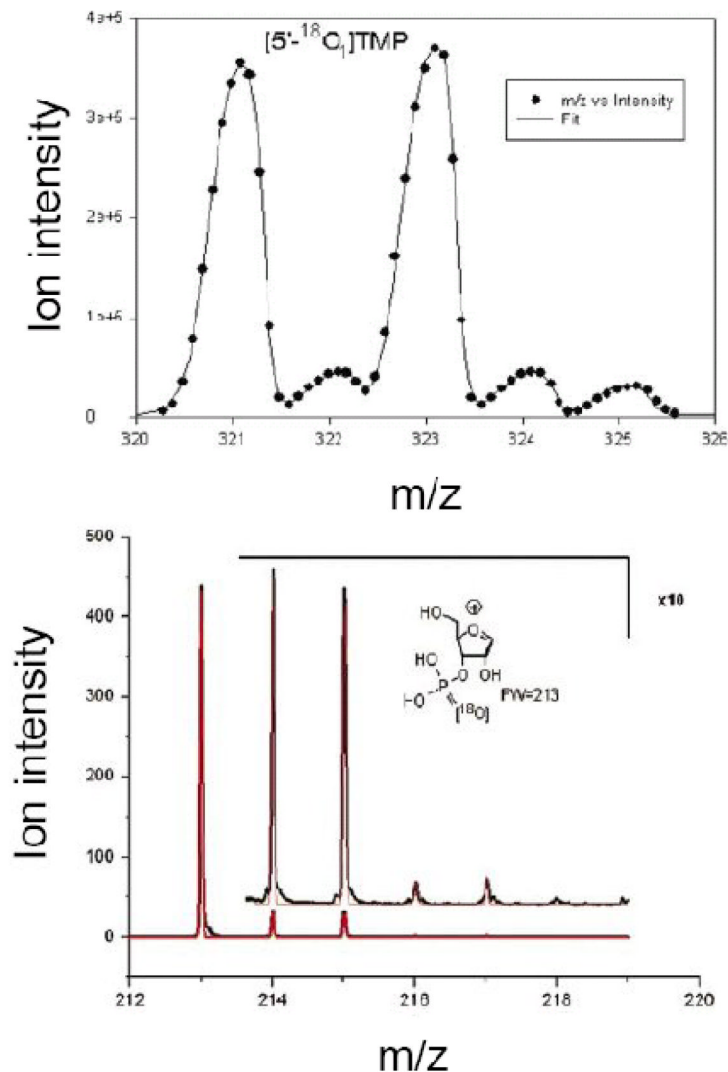


Figure 8. Positions of diester reactions on a MOJ landscape as suggested by the magnitudes of $^{18}k_{\text{NUC}}$ and $^{18}k_{\text{LG}}$, for alkaline hydrolysis of model phosphodiester. The orientation of the MOJ landscape is the same as in Figure 2. The positions of reaction TS (circles) are approximate as they are depicted as defined here solely by the magnitude of the observed ^{18}k values linearly reflecting bond order. It is recognized that additional factors such as differences in the vibrational states of intra versus intermolecular reactions and contributions from proton transfer and metal ion coordination do necessarily contribute to the magnitude of the observed KIEs. As indicated in the text additional computational analyses and investigation of model reactions will be necessary to accurately relate the observed nucleophile and leaving group KIEs in terms of absolute bond order. The diesters examined are designated as in Figure 7.

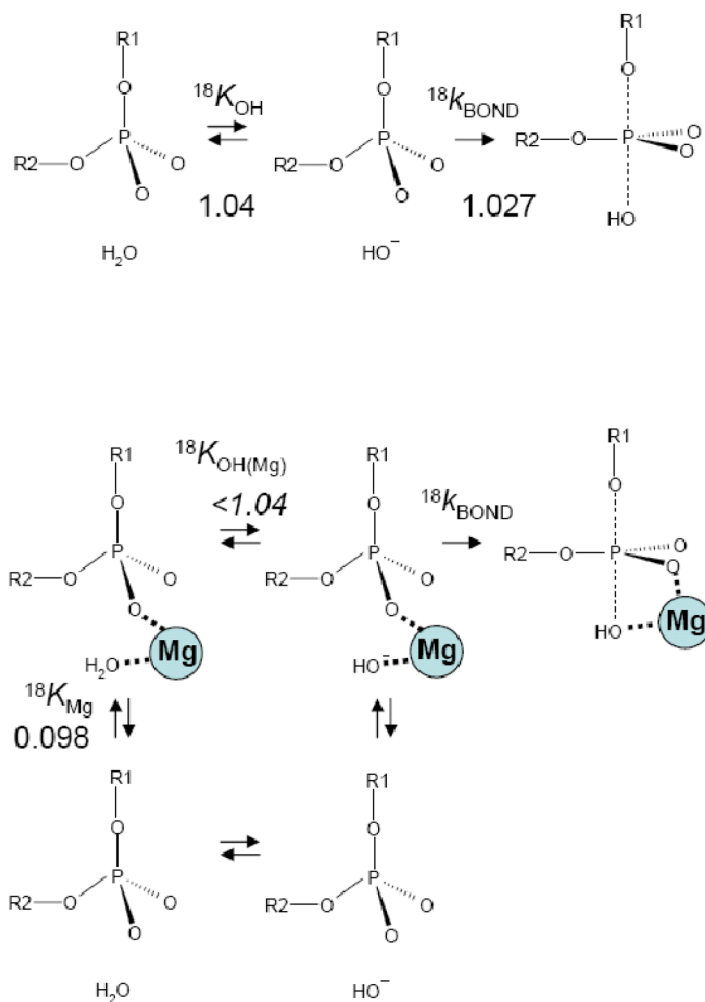


Figure 9. Mechanistic interpretation of nucleophile kinetic isotope effects for Mg^{2+} catalysis of T-5'-pNPP hydrolysis and RNA hydrolysis catalyzed by P RNA. Model for nucleophilic activation by the RNase P ribozyme and effects of direct coordination by Mg^{2+} on the observed $^{18}k_{\text{NUC}}$. Coordination of water by Mg^{2+} exhibits an inverse (0.98) isotope effect ($^{18}K_{\text{Mg}}$). Magnesium will also perturb the equilibrium isotope effect on deprotonation of water to form hydroxide ($^{18}K_{\text{OH}}$), resulting in a similar inverse shift in the observed effect. As discussed in the text it is also possible that metal ion interactions can alter the intrinsic kinetic isotope effect for bond formation ($^{18}k_{\text{bond}}$).